Supplementary information

Uncovering the critical function of lanthanum in CH_4 production from CO_2 using exsolved $LaNiO_3$ perovskite catalysts

Mathias Barreau[a,*], Davide Salusso[b], Jinming Zhang[a], Michael Haevecker[c,d], Detre Teschner[c,d], Anna Efimenko[e,f], Fabrice Bournel[g,h], Jean-Jacques Gallet[g,h], Elisa Borfecchia[i], Kamil Sobczak[j], Corinne Petit[a] and Spyridon Zafeiratos[a,*]

[a]*Institut de Chimie et Procédés pour l'Energie, l'Environnement et la Santé (ICPEES), ECPM, UMR 7515 CNRS – Université de Strasbourg, 25 rue Becquerel, 67087 Strasbourg Cedex 02, France*

[b]*European Synchrotron Radiation Facility, CS 40220, Cedex 9 F-38043 Grenoble, France*

[c]*Max-Planck-Institut für Chemische Energiekonversion (MPI-CEC), Stiftstrasse 34-36, D-45470 Mülheim a.d. Ruhr, Germany*

[d]*Fritz-Haber-Institut der Max-Planck-Gesellschaft, Faradayweg 4-6, D-14195 Berlin, Germany*

[e]*Interface Design, Helmholtz-Zentrum Berlin für Materialien und Energie GmbH (HZB), Albert-Einstein-Str. 15, 12489 Berlin, Germany*

[f]*Energy Materials In-situ Laboratory Berlin (EMIL), Helmholtz-Zentrum Berlin für Materialien und Energie GmbH (HZB), Albert-Einstein-Str. 15, 12489 Berlin, Germany*

[g]*Laboratoire de Chimie Physique-Matière et Rayonnement, Sorbonne Universite´, Campus Curie, CNRS UMR 7614, 4 place Jussieu, 75005 Paris, France*

[h]*Synchrotron SOLEIL, L'orme des Merisiers, B.P. 48, Saint Aubin, Gif-sur-Yvette Cedex 91192, France*

[i]*Department of Chemistry, INSTM Reference Center and NIS Centers, University of Torino, 10125 Torino, Italy*

[j]*Faculty of Chemistry, Biological and Chemical Research Centre, University of Warsaw, Zwirki, Wigury 101, 02-089 Warsaw, Poland*

Corresponding Authors

*mbarreau@unistra.fr; *spiros.zafeiratos@unistra.fr

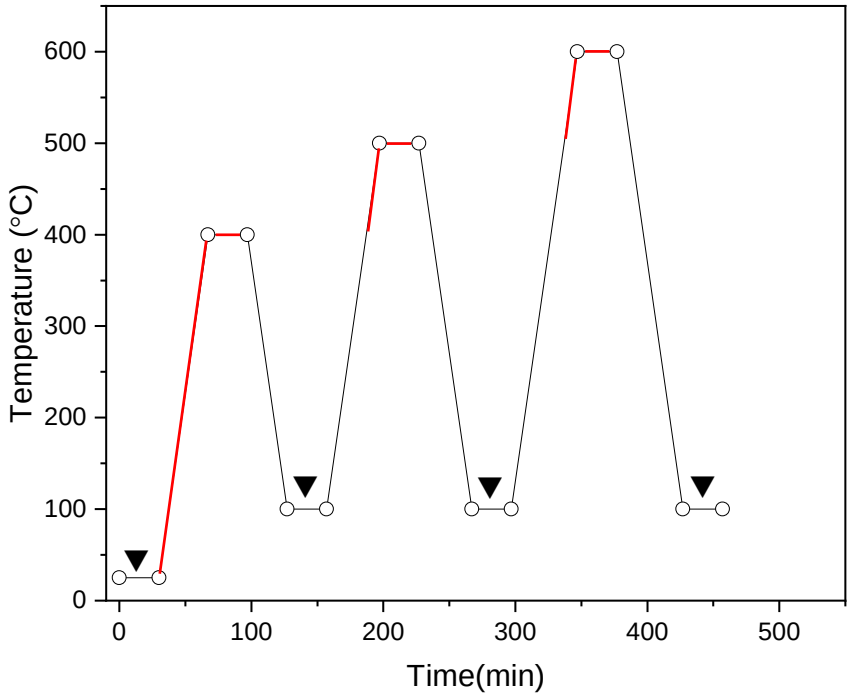

Figure S 1. Scheme of the temperature protocol employed for the *in-situ* XAS experiment. Measurements were performed during ramping and steady state (red line) as well as after cooling at 100 °C (triangles).

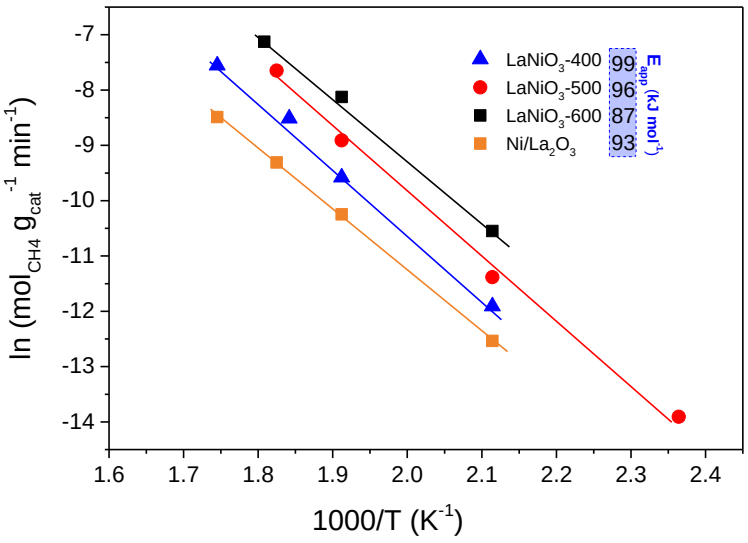

Figure S 2 Arrhenius plots and the deduced apparent activation energies (E_{app}) of $LaNiO_3$ catalyst subjected to H_2-activation pretreatment at 400, 500 and 600 °C for 30 min. The corresponding E_{app} of supported Ni/La_2O_3 catalysts pretreated at 600 °C in H_2 is included for comparison.

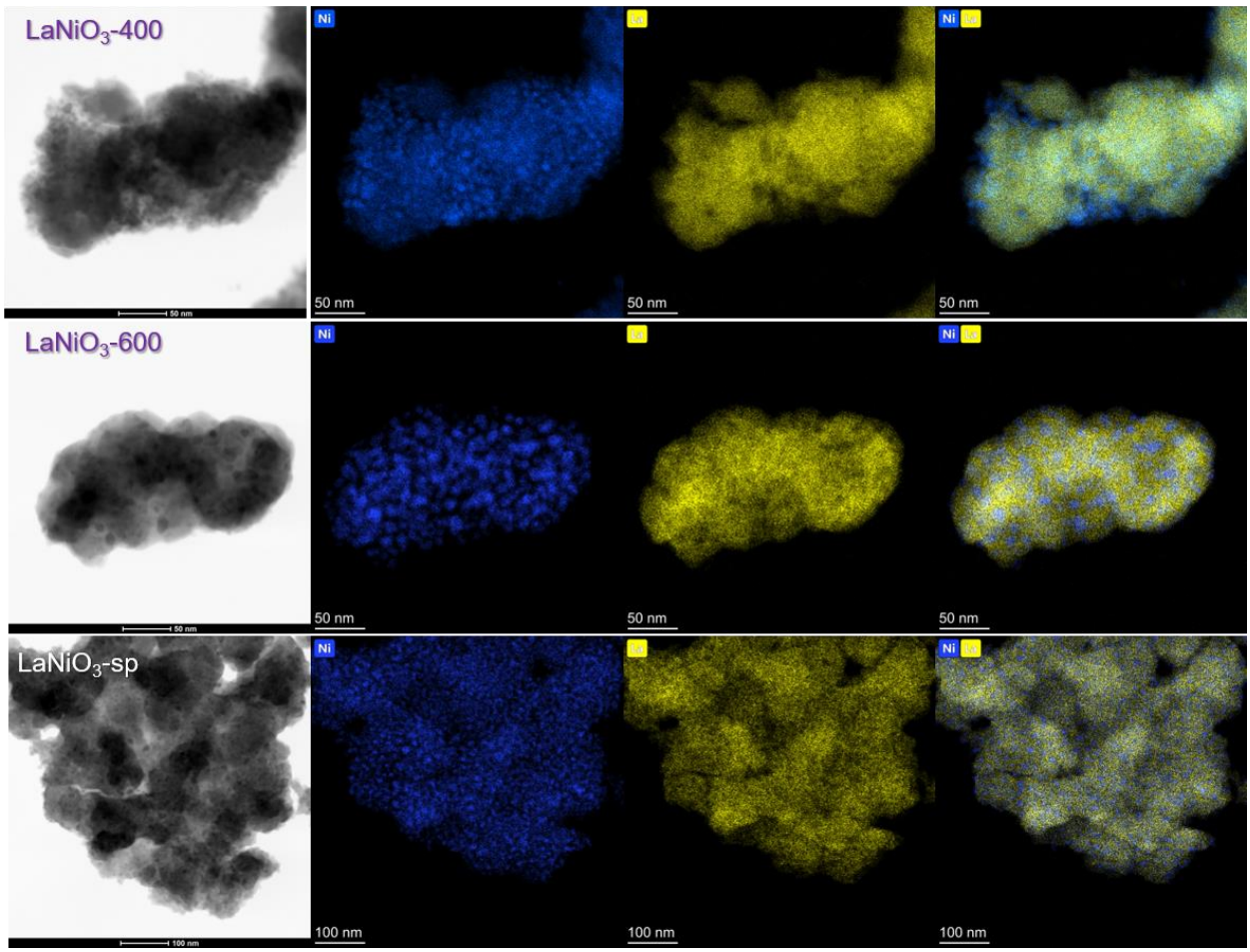

Figure S 3. TEM images and EDX elemental mapping of $LaNiO_3$-400, $LaNiO_3$-600 and $LaNiO_3$-sp catalysts

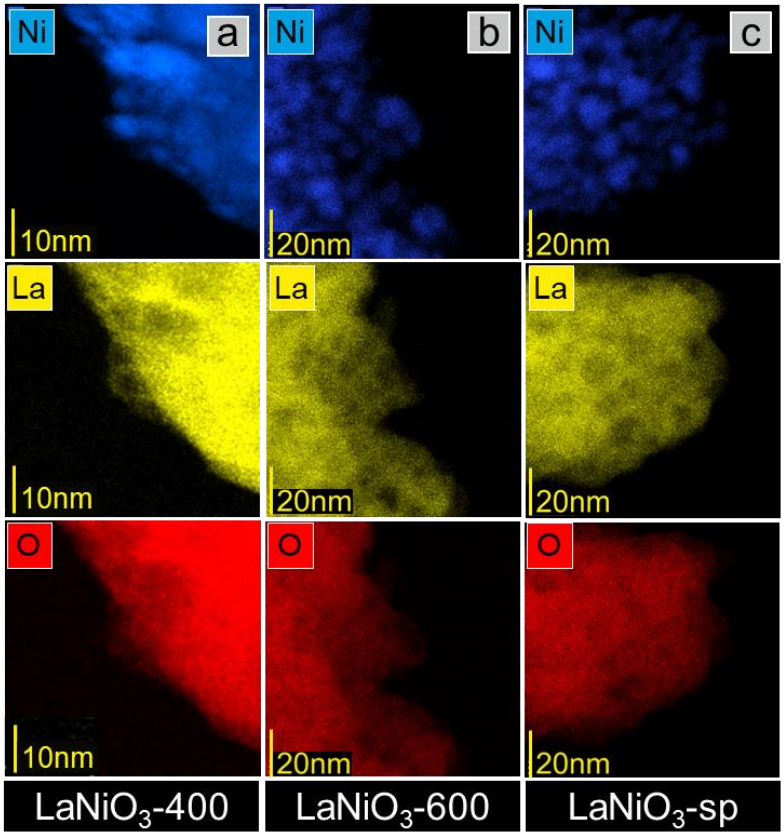

Figure S 4. Isolated elemental O, Ni and La mapping of $LaNiO_3$-400, $LaNiO_3$-600 and $LaNiO_3$-sp catalysts.

Details about the ex-situ XANES spectra analysis

The Ni K-edge of fresh $LaNiO_3$ catalysts shown in Figure 4, resembles very much that of reference $LaNiO_3$ in accordance with the XRD results of Figure 2 in the main text. After H_2-activation and catalytic tests the Ni K-edge of both $LaNiO_3$ and Ni/La_2O_3 show a clear increase of a broad component in the rising edge centered at 8337 eV (component B in Figure 4a), combined with an important decrease of white-line peak intensity and post-edge oscillations amplitude, characteristic of metallic Ni^0 formation. In parallel, the white-line peak shifts to lower energies which is a sign of potential NiO presence (component C in Figure 4a). The partial reduction of $LaNiO_3$ to Ni^0 is confirmed by the FT-EXAFS spectra in Figure S5, showing the appearance of Ni-Ni single scattering path from Ni^0 (Ni-Ni_{Ni}) at the detriment of Ni-La one. A second Ni-Ni path at around 2.5 Å (phase uncorrected) is associated to the NiO phase.

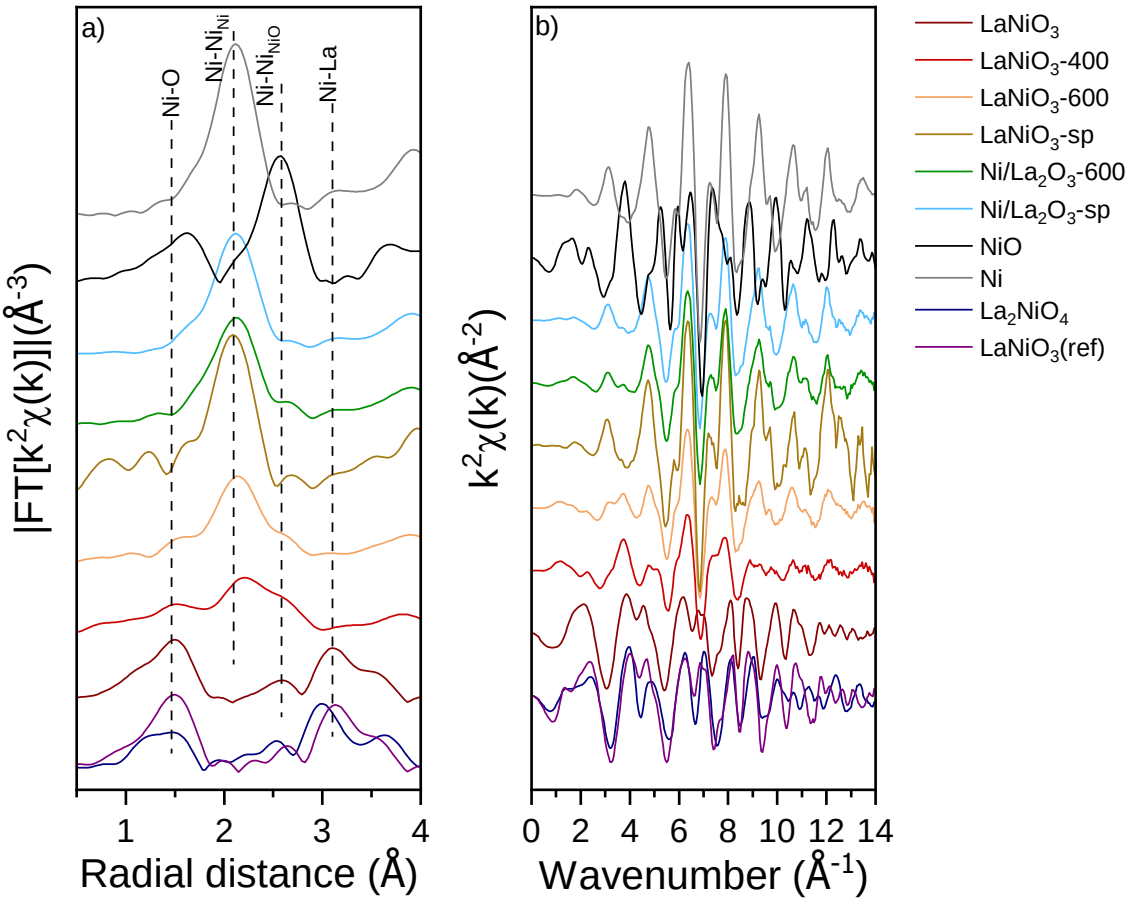

Figure S 5. (a) Magnitude of Ni K-edge phase uncorrected FT-EXAFS spectra for Ni-catalysts and relevant model compounds investigated in this work. **(b)** Corresponding k^2-weighted χ(k) EXAFS spectra.

Linear Combination Analysis (LCA) of the Ni K-edge using reference spectra from NiO, Ni, $LaNiO_4$ and $LaNiO_3$ samples (Figure S6) suggest the presence of 84% $LaNiO_3$, 12% La_2NiO_4 and 2% NiO phases (see also Figure 4b). Even though the latter is close to the technique sensitivity, it was previously reported that amorphous nanosized NiO might be formed during $LaNiO_3$ synthesis; hence we cannot exclude its minority presence.[1,2]

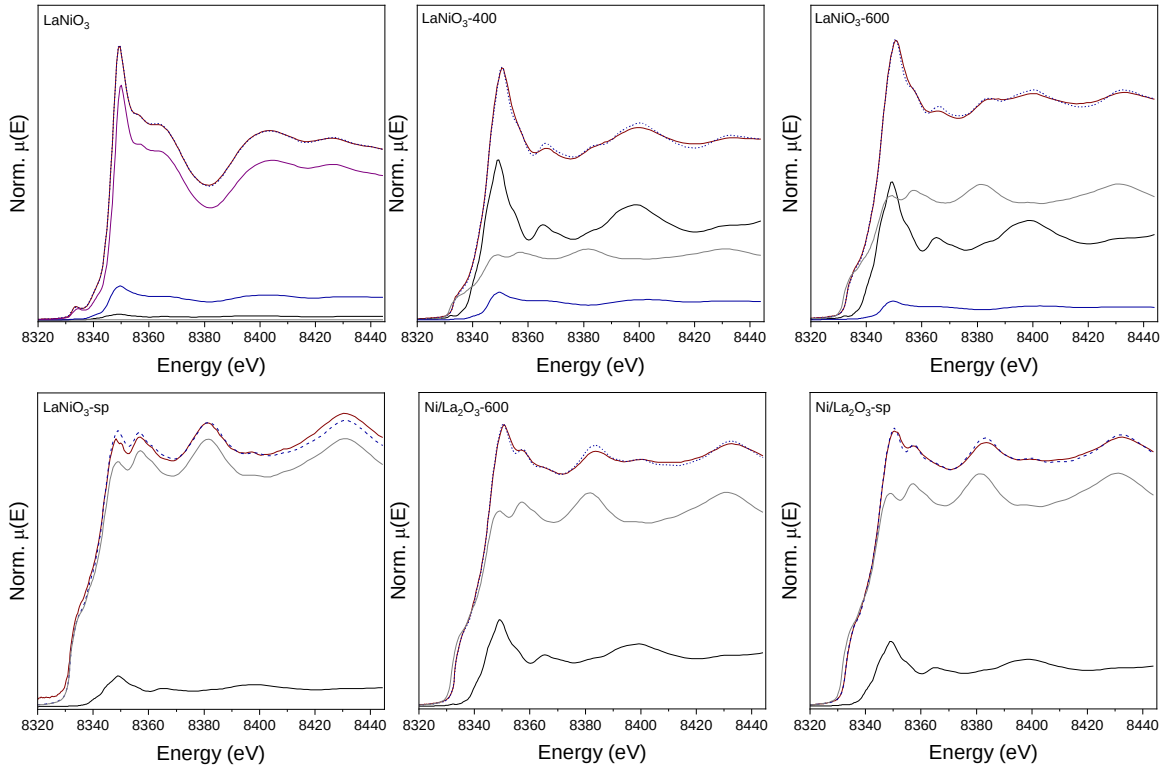

Figure S 6. Ni K-edge XANES experimental spectra (red line), LCA best fit (dashed blue line) and weighted Ni^0 (grey line), NiO (black line) and La_2NiO_4 (blue line) components.

The FT-EXAFS spectra were fitted considering the components evaluated by LCA procedure (Figure S7b). As reported in Table S1, the relative abundance of NiO and Ni^0 phases in the fitting was fixed according to the LCA results. Due to its low concentration (< 15%) the La_2NiO_4 phase was not considered in the fitting. The FT-EXAFS fit gives physically reliable Debye Waller (DW) values (Table S1) for Ni-La single scattering (SS) paths of all spectra apart from fresh/calcined $LaNiO_3$. In the latter, fit leads to unphysical DW values despite the existence of Ni-La SS paths is confirmed from EXAFS Wavelet Transform 2D plots (Figure S7c), showing a contribution at high R and k-ranges, and comparison with $LaNiO_3$ reference spectra (Figure S5). It is noteworthy the broad contribution centered at 2.75 Å/5 $Å^{-1}$ (R/k) related to Ni-O-O intense double scattering (DS) typical of La_2NiO_4 and $LaNiO_3$ as observable from references in Figure S8. As shown in Figure S7b, the fit curves describe well the experimental spectra indicating that the lower intensity of Ni^0 in the Ni-Ni first coordination shell is not related to particle size but rather to phase concentration (i.e., the amount of Ni^0). As per the FT-EXAFS fit results (refer to Table S1), it is evident that both $LaNiO_3$ and Ni/La_2O_3 catalysts exhibit metallic and oxidized Ni particles with coordination numbers characteristic of bulk-like structures.

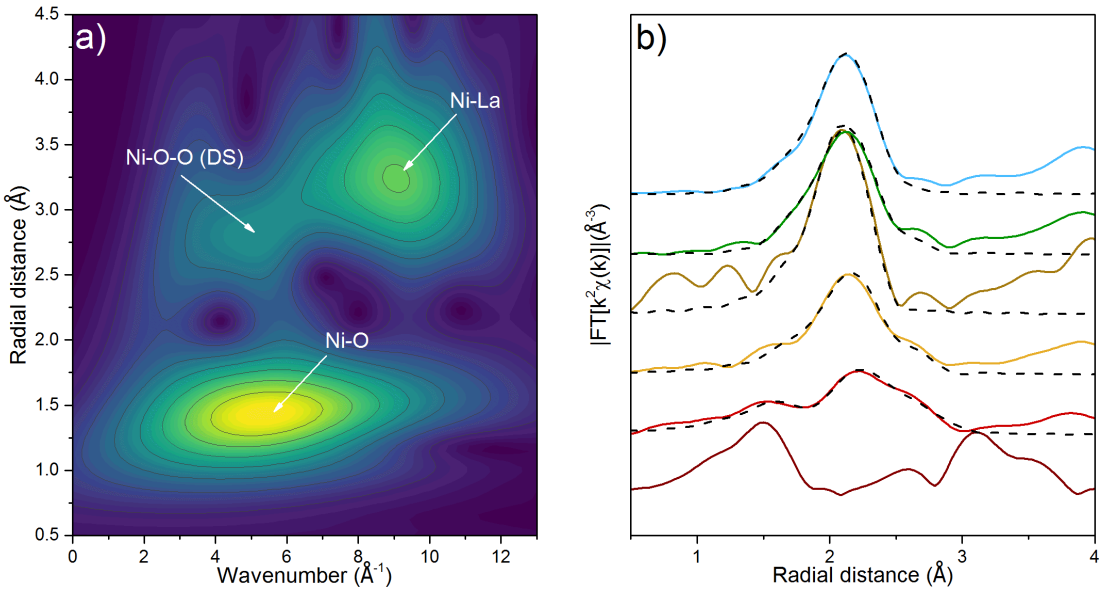

Figure S 7. (a) Full range EXAFS Wavelet Transform 2D plots of $LaNiO_3$ collected at room temperature. **(b)** FT-EXAFS spectra of $LaNiO_3$ and Ni/La_2O_3 together with their best fit curved (dashed lines)

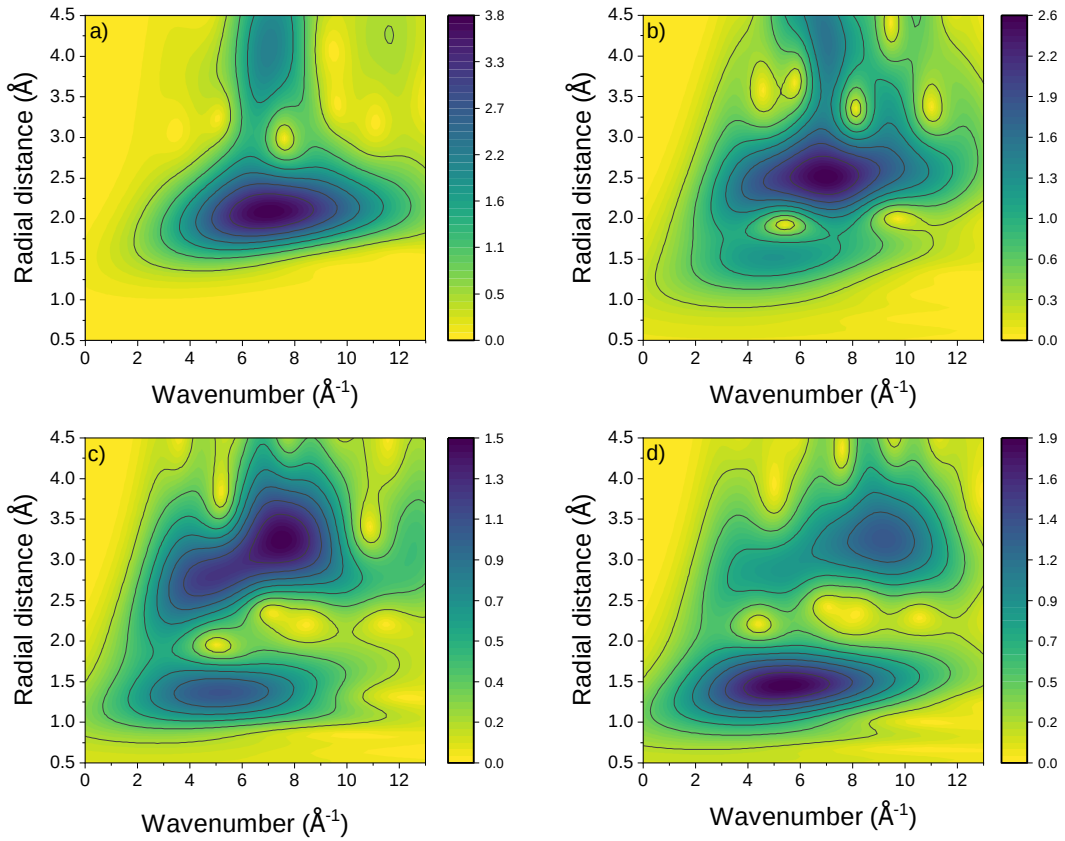

Figure S 8. Full range EXAFS Wavelet Transform 2D plots of reference a) Ni, b) NiO, c) La_2NiO_4 and d) $LaNiO_3$.

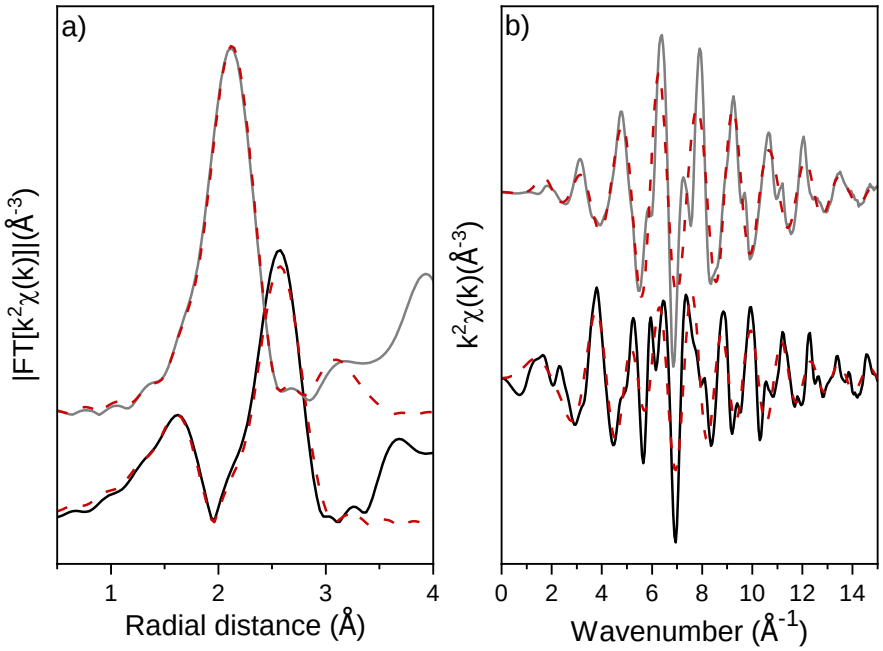

Figure S 9. (a) Magnitude of FT-EXAFS and **(b)** k^2-weighted χ(k) EXAFS experimental spectra of NiO (black line) and Ni^0 (grey line). Best fit curves are reported as dashed red lines.

Table S 1. Results of FT-EXAFS fit of reference NiO, Ni^0 together with $LaNiO_3$ and Ni/La_2O_3 catalysts.

	NiO	Ni	$LaNiO_3$-400	$LaNiO_3$-600	$LaNiO_3$-sp	Ni/La_2O_3	Ni/La_2O_3-sp
R factor	0.012	0.023	0.008	0.019	0.02	0.015	0.010
$N_{var}(N_{ind})$	5(15)	6(18)	7(12)	7(13)	4(8)	7(13)	7(13)
ΔE (eV)	-3.50± 0.08	-6.1 ± 1.2	-2.5 ± 1.1	-5 ± 2	-9.3 ± 1.9	-6.6 ± 1.8	-7.1 ± 1.8
S_0^2	0.82*	0.82 ± 0.08	0.82*	0.82*	0.82*	0.82*	0.82*
R-range	1 – 3.2	1 – 3.7	1 – 3	1 – 3	1.4 – 2.7	1 - 3	1 – 3
k-range	3 – 14	3 - 14	2.5 - 13	2.5 - 13	3 - 14	3 – 14	3 - 14
CN(Ni-O)	6	/	6 x NiO_{LCA}	6 x NiO_{LCA}	/	6 x NiO_{LCA}	6 x NiO_{LCA}
R(Ni-O)(Å)	2.075 ± 0.009	/	2.062 ± 0.010	2.03 ± 0.02	/	2.05 ± 0.03	2.04 ± 0.05
σ(Ni-O)($Å^{-2}$)	0.0051 ± 0.0009	/	0.0054 ± 0.0011	0.006 ± 0.002	/	0.004 ± 0.003	0.006 ± 0.007
CN(Ni-Ni)	12	12					
R(Ni-Ni)(Å)	2.953 ± 0.005	2.484 ± 0.006	M				
σ(Ni-Ni)($Å^{-2}$)	0.00557 ± 0.0003	0.00862 ± 0.0007					
CN(Ni-Ni)	/	6					
R(Ni-Ni)(Å)	/	3.49 ± 0.02					
σ(Ni-Ni)($Å^{-2}$)	/	0.008 ± 0.002					
$CN(Ni\text{-}Ni)_{NiO}$ $CN(Ni\text{-}Ni)_{Ni}$	/	/	12 x NiO_{LCA} 12 x Ni_{LCA}	12 x NiO_{LCA} 12 x Ni_{LCA}	/ 11.7 ± 1.8	12 x NiO_{LCA} 12 x Ni_{LCA}	12 x NiO_{LCA} 12 x Ni_{LCA}
$R(Ni\text{-}Ni)_{NiO}$(Å) $R(Ni\text{-}Ni)_{Ni}$(Å)	/	/	2.988 ± 0.012 2.509 ± 0.007	2.96 ± 0.02 2.496 ± 0.012	/ 2.469 ± 0.009	2.95 ± 0.04 2.486 ± 0.010	2.89 ± 0.09 2.488 ± 0.008
$\sigma(Ni\text{-}Ni)_{NiO}(Å^{-2})$ $\sigma(Ni\text{-}Ni)_{Ni}(Å^{-2})$	/	/	0.0113 ± 0.0008 0.0082 ± 0.0005	0.012 ± 0.002 0.0073± 0.0005	/ 0.0059 ± 0.0011	0.012 ± 0.004 0.0076 ± 0.0004	0.019 ± 0.018 0.007± 0.003

**indicates values that were fixed. Fit were conducted in the reported R and k ranges.*

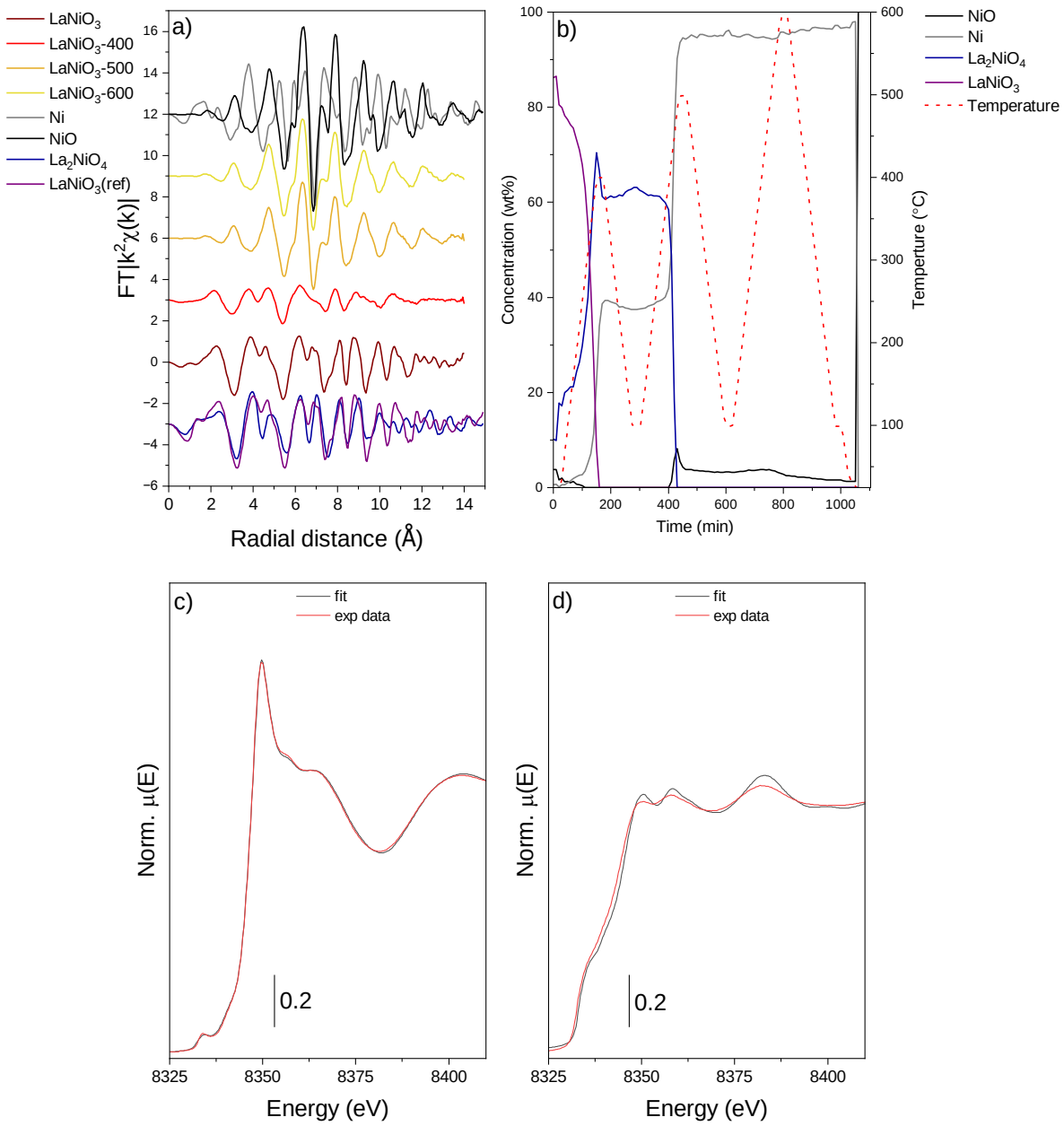

Figure S 10. **(a)** Ni K-edge k^2-weighted χ(k) EXAFS spectra. **(b)** LCA concentration results obtained on the whole protocol analysis. Temperature is indicated with dashed red line. **(c)** LCA best fit (black line) compared with its corresponding experimental spectra (red line). **(d)** LCA worst fit (black line) compared with its corresponding experimental spectra (red line).

Details about the combined curve fitting of La3d and Ni 2p AP-XPS spectra

The Ni 2p and La 3d spectra were fitted together by a combination of peak line-shapes derived from reference materials mathematical formulas, as indicated in the caption of the figure below. Several constrains were applied regarding the relative BE positions and peak area ratio between the peaks as well as the FWHM of those peaks. The independent parameters of the fitting were the BE position of La $3d_{5/2}$ and Ni^0 peaks as well the area of the various components. These parameters were allowed to vary up to the minimization of the residual standard deviation (RSD), typically kept below 2. To note that the same constrains were applied to the fitting of all Ni2p&La3d spectra independent of the excitation photon energy used.

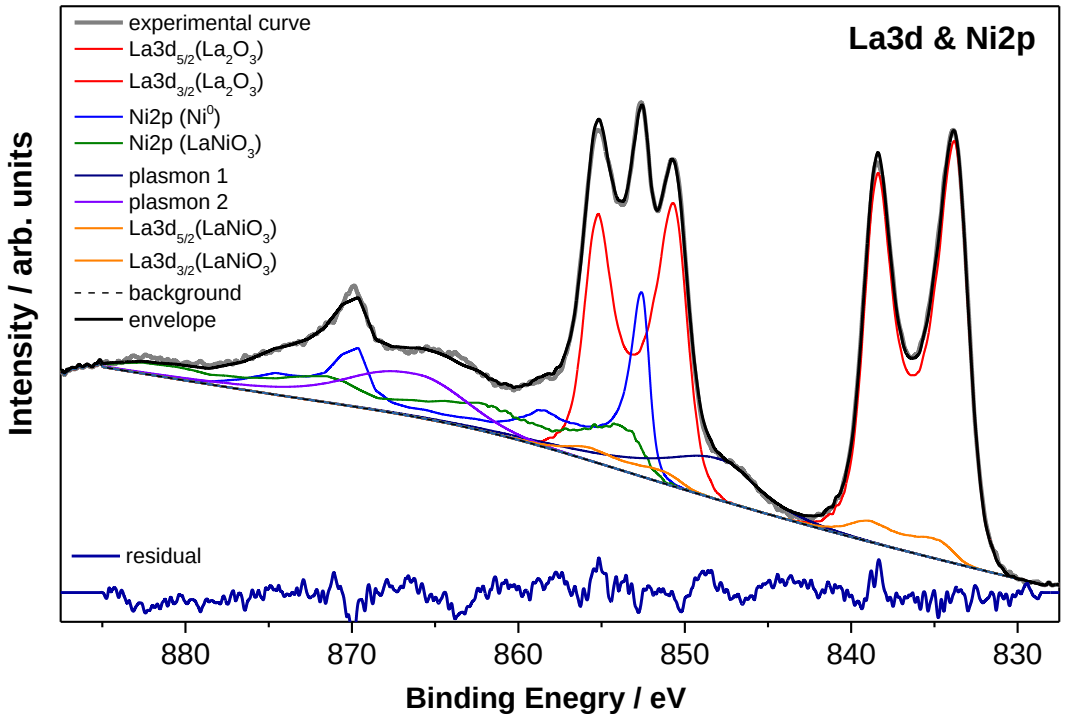

Figure S 11. Example of Ni 2p and La 3d spectra curve fitting using peak line-shapes derived from reference materials (La_2O_3, $LaNiO_3$, Ni^0) and synthetic asymmetric line-shape derived by a mathematical formula (plasmon 1 and 2 peaks). A spline-Shirley background type was used. The following constraints were applied in the fitting. **(A)**: Area constraints : the ratio between La $3d_{5/2}$ and La $3d_{3/2}$ peaks was fixed to 3:2, the ratio between plasmon 1 and 2 peaks was fixed to 1.2, **(B)**: Binding Energy constraints: the separation between La $3d_{5/2}$ and La $3d_{3/2}$ peaks was fixed to 16.9 eV, the separation between plasmon 1 and 2 peaks was 16.8 (±0.2) eV, the separation between the Ni 2p peaks of Ni^0 and $LaNiO_3$ was 1.7 (±0.2) eV, the separation between the La 3d peaks of La_2O_3 and $LaNiO_3$ was 5.0 (±0.2) eV. **(C)**: Full width at half maximum (FWHM) constraints: The FWHM of the peaks derived from reference materials was fixed to 1.00 (±0.02) eV. Residual is displayed below the spectrum.

In the fitting of the Ni2p&La3d spectra measured under reaction conditions (Figure 7) the La $3d_{5/2}$ peak could not be fitted properly by the La_2O_3 and $LaNiO_3$ reference peaks. Therefore an additional synthetic line-shape was used to fit Ni2p&La3d spectra under reaction conditions. The characteristics of the synthetic La 3d peak are given in Table S2.

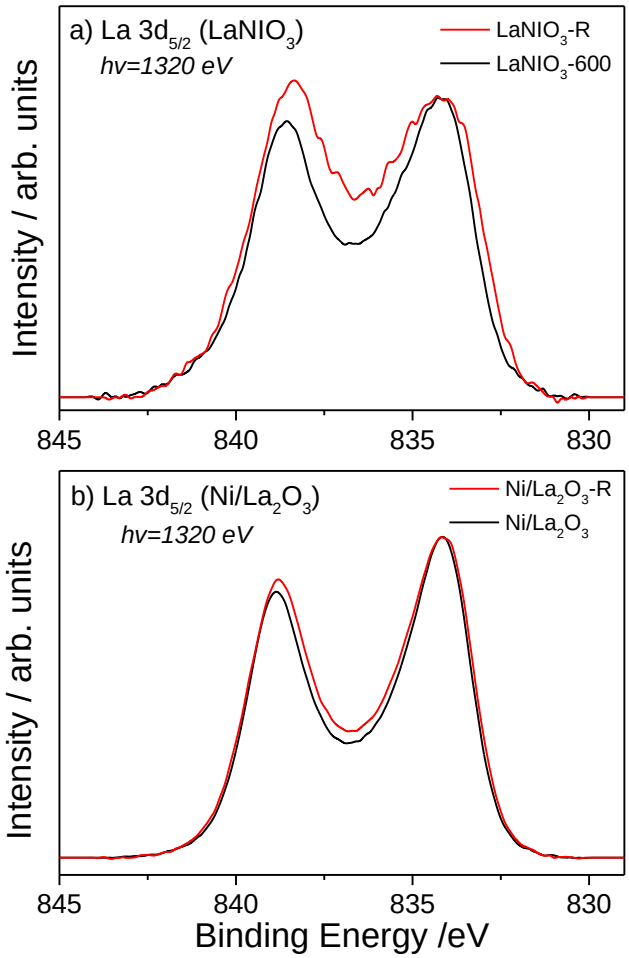

Figure S 12. Comparison of the AP-XPS La $3d_{5/2}$ photoemission peaks recorded with the catalysts in reduction (2 mbar H_2, 400 °C; black lines) and CO_2 methanation reaction (2 mbar CO_2:H_2 (1:1), 400 °C; red lines) conditions for **(a)** $LaNiO_3$-600 and **(b)** Ni/La_2O_3 catalyst. In order to facilitative their comparison, the spectra are shown after linear background subtraction and normalization to the same height.

Table S 2. Parameters of the synthetic La 3d peak components (abbreviated as s.La 3d) used for the curve fitting of the Ni2p&La3d spectra measured under reaction conditions (Figure 7).

	La $3d_{5/2}$		La $3d_{3/2}$	
	Main peak	Satellite peak	Main peak	Satellite peak
Line shape	GL(50)T(1.1)	GL(50)	GL(50)T(1.1)	GL(50)
BE	834.7 (±0.1) eV	La $3d_{5/2}$-3.5(±0.1) eV	La $3d_{5/2}$-16.8(±0.1) eV	La $3d_{3/2}$-3.5(±0.1) eV
Area	N/A	La $3d_{5/2}$*0.58	La $3d_{5/2}$*0.67	La $3d_{3/2}$*0.58

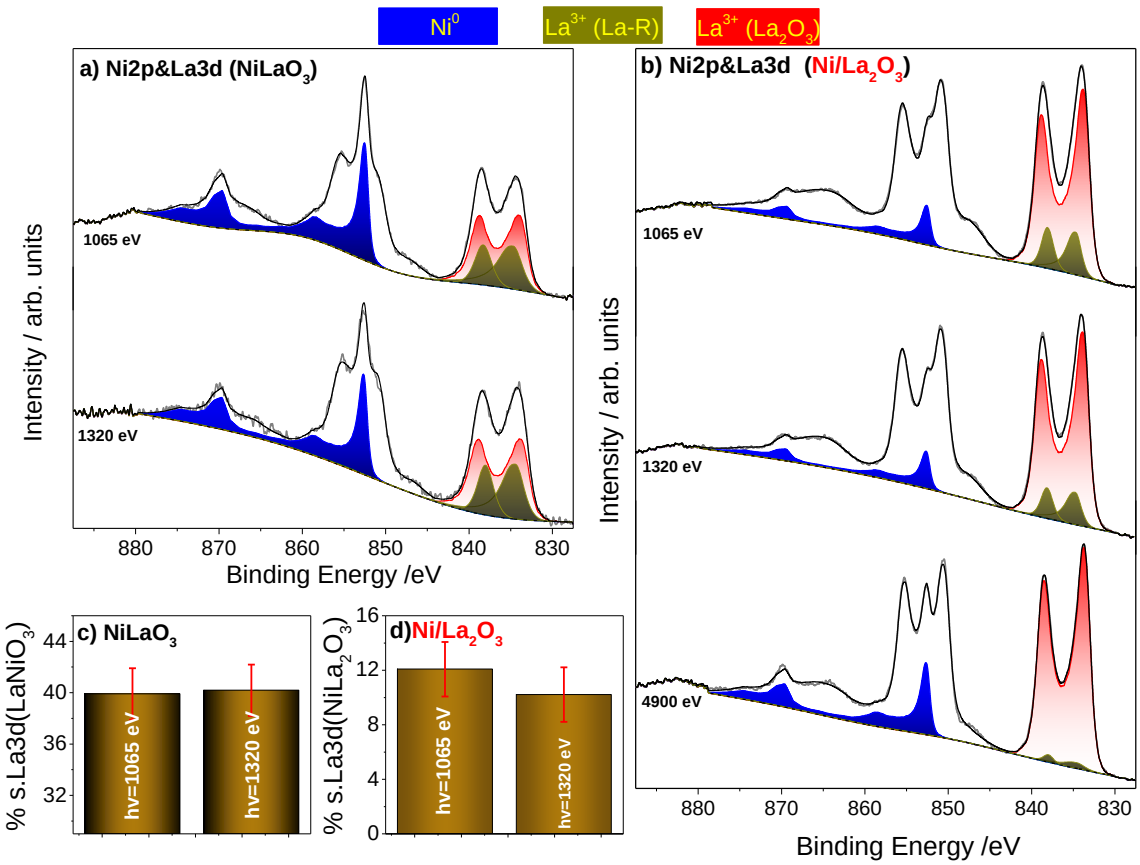

Figure S 13. *In-situ* depth-dependent La 3d and Ni 2p spectra of **(a)** $LaNiO_3$-600 **(b)** Ni/La_2O_3 catalysts measured under CO_2 methanation conditions (2 mbar CO_2:H_2 (1:1) at 400 °C). The excitation energies are indicated under each spectrum. For clarity, only the La $3d_{5/2}$ and Ni 2p fitting components are shown. Bar graph showing the % La atomic concentration at 2 information depths (2.4 and 3.9 nm) for **(c)** $LaNiO_3$-600 **(d)** Ni/La_2O_3 catalysts calculated by the Ni 2p and La 3d peak areas of the spectra shown in (a) and (b).

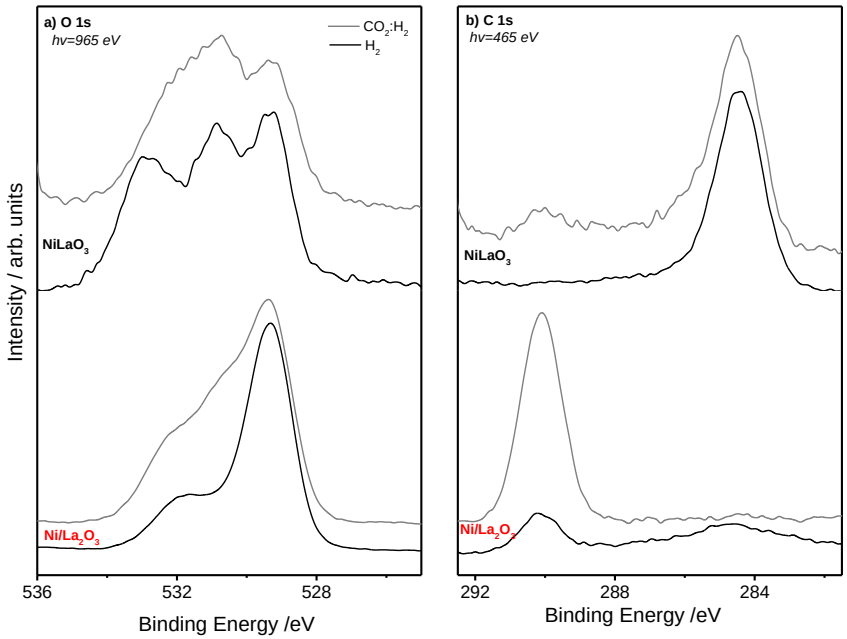

Figure S 14. *In-situ* **(a)** O 1s and **(b)** C 1s spectra of $LaNiO_3$-600 and Ni/La_2O_3 catalysts measured in H_2 (black line) and CO_2:H_2 (gray lines) atmospheres. The excitation energies are indicated at the top.

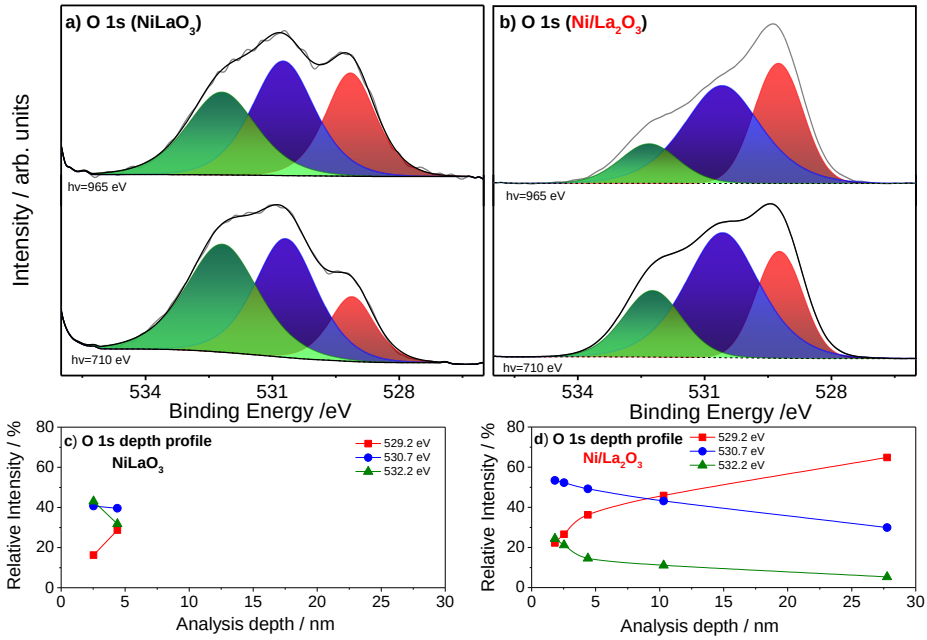

Figure S 15. *In-situ* depth-dependent O 1s spectra of **(a)** $LaNiO_3$-600 **(b)** Ni/La_2O_3 catalysts measured under CO_2 methanation conditions (2 mbar CO_2:H_2 (1:1) at 400 °C). The excitation energies are indicated under each spectrum. The spectra are fitted by 3 O 1s symmetric peaks, corresponding to 3 different oxygen species. **(c)** The evolution of relative concentration of each oxygen species (i.e. O 1s peak) as a function of the analysis depth (i.e. 3 times the photoelectrons inelastic mean free path) for the Ni/La_2O_3 catalysts.

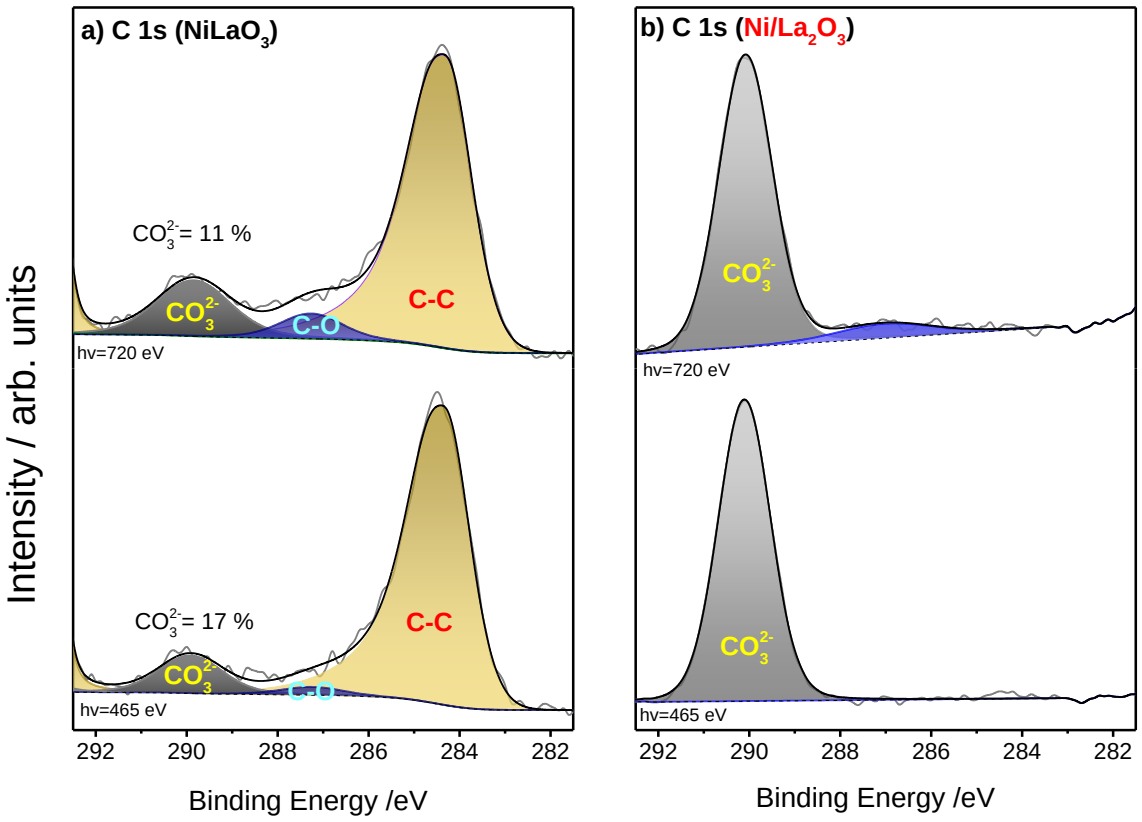

Figure S 16. *In-situ* depth-dependent C 1s spectra of **(a)** $LaNiO_3$-600 **(b)** Ni/La_2O_3 catalysts measured under CO_2 methanation conditions (2 mbar CO_2:H_2 (1:1) at 400 °C). The excitation energies are indicated under each spectrum. The $LaNiO_3$-600 sample spectra are fitted by one asymmetric C 1s peak due to C-C species, together with 2 symmetric peaks for C-O and CO_3^{2-} species. For the fitting of Ni/La_2O_3 sample spectra only 2 peaks due to C-O and CO_3^{2} were necessary. The % represents the fraction of CO_3^{2-} species to the overall C 1 s peak.

References

(1) Pereñiguez, R.; Gonzalez-delaCruz, V. M.; Caballero, A.; Holgado, J. P. *Appl. Catal. B Environ.* **2012**, *123–124*, 324–332.

(2) Liu, L.; Zhang, Z.; Das, S.; Xi, S.; Kawi, S. *Energy Convers. Manag.* **2020**, *206*, 112475.